Evaluation of Three-Axis Magnetic Loop Antenna Cross Coupling for Low-Frequency Measurements

Denys Pokotilov[1]
[1]*University of Twente*
Enschede, The Netherlands
denys.pokotilov@utwente.nl

Robert Vogt-Ardatjew[1]
[1]*University of Twente*
Enschede, the Netherlands

Frank Leferink[1,2]
[1]*University of Twente*
Enschede, the Netherlands
[2]*Thales, Nederland B.V.*
Hengelo, The Netherlands

***Abstract* — Nowadays the majority of electrical devices are complex systems with different operation modes and switching elements. The amount of evaluation procedures that are needed to be done for these devices increases drastically. It is pushing standard radiated EMI measurements to the edge, where the advantage between time and the accuracy of measurements should be chosen. Standard low-frequency measurements as CISPR 36, used to evaluate radiated EMI for frequencies below 30 MHz, became too time-consuming and expensive. Proposed improvements which include time-domain multichannel measurements in combination with a three-axis shielded loop antenna can be more time-efficient. Compared to a conventional single-loop antenna, one of the potential challenges is the coupling between loops for the two- and three-axis antenna. This paper investigates the effect of coupling between the individual loops when illuminated with a complex field, which is shown to be the worst-case scenario. Only some minor coupling is observed implying that such a three-axis loop antenna can be used without sacrificing much accuracy, while still providing a significant improvement in the measurement time-efficiency.**

Keywords — Three-axis antenna, EMI measurements, multichannel, coupling, low-frequency measurements

I. INTRODUCTION

Low-frequency electromagnetic (EM) emission measurements of modern equipment under test (EUT) can be time consuming. Electrical vehicles [1], [2], [3], wind turbines [4], and a lot of other devices need to be evaluated at multiple sides during different working modes, and with several antennas directions. In some cases, it can only be performed outdoors, which leads to more complex and time-consuming measurements due to the weather condition, etc. [5]. Several possibilities to reduce the measurement time were studied [6]. Multi-channel time-domain measurements already provide considerable time reduction [7]. As an alternative of one single shielded loop antenna, the multi-axis antenna, made of three orthogonal loops, has been used by amateur radio for several decades [8]. Van Veen introduced a loop antenna for EM emission measurements, which includes three orthogonal loops, for evaluation of small EUT [9]. The possibility to use three orthogonal loop 60 cm antennas has been investigated in [7], [10]. The combination of multi-axis antenna and multichannel measurement device could provide the evaluation of EM field in three orientations simultaneously. Because these loop antennas are placed in close proximity, the mutual coupling which will be created should be taken into account. In [2] the coupling between two orthogonal shielded loop antennas using basic evaluation procedure with directional reference EM field source was shown.

Modern EUT can radiate EMI in several directions and polarizations at the same time. In [3] it is clearly visible that the EM propagation in two different axis is almost the same. Due to this the possibility that the EUT would radiate and in the third axis, with the same level is present. Although not done currently, in the future, it could lead to increasing the number of measured polarizations from two to three which should be taken into consideration. Standard method for antenna factor measurement [11] to quantify uncertainty in the measurement results between one- and two-antenna construction was used. During the measurements directional EM field from the transmitting antenna was used. In this case the highest mutual coupling which could be caused by two-antenn*a* construction would be underestimated due to the cross-polarization factor. It comes from the fact that with a polarized EM field one of the orthogonal antennas is dominant. In [12] a simple example of two perpendicular wires, which can be compared to the orthogonal shielded antennas, was investigated. It shows that, even when keeping the perpendicular position of the wires, the cross-coupling is present and it is stronger with a higher signal in both wires. In this case, if each orthogonal antenna in the two-antenna construction is exposed to the fields of similar magnitudes it could lead to the unwanted measurement error of the radiated EM field. With the increasing number of orthogonal antennas from two to three, the severity of the cross-coupling between each antenna is expected to increase. Therefore, the evaluation procedure to determine the impact on the measurement results due to the presence of the extra antennas should be investigated deeper in order to validate its usability for EMC testing

In this paper, the mutual coupling between the loops of a two- and three-axis orthogonal antennas is investigated. The perfect-case scenario based on the standard method [11] using a single antenna is compared to the two- and three-antenna constructions. To verify the highest error which could be caused by the presence of an additional antennas based on [13], the EM field should contain all three polarizations with the same level. To be able to achieve nearly the same EM field in three polarizations simultaneously the transmitting antenna was tilted in each of three-axes. Using this measurement, the correction factor, which is based on the measured field of each antenna, could be calculated. The better scenario would however be a three-antenna method in the standards, instead of introducing some corrections between a one-, a two- or a three-antenna sensor.

ETOPIA project research is funded by the European Union's Horizon 2020 research and innovation programme under the Marie Sklodowska Curie grant agreement No 812753

2022 IEEE International Symposium on Electromagnetic Compatibility & Signal/Power Integrity (EMCSI) | 978-1-6654-0929-2/22/$31.00 ©2022 IEEE | DOI: 10.1109/EMCSI39492.2022.9889631

II. Three-axis antenna construction

In Fig. 1 the antenna positions around a car for standard radiated EMI measurements according to CISPR 36 [14], [15] are shown. All positions and orientations result in 8 measurements because two antenna orientations are used in each position. Despite a small number of measurements, complete measurement procedure takes around 10 hours.

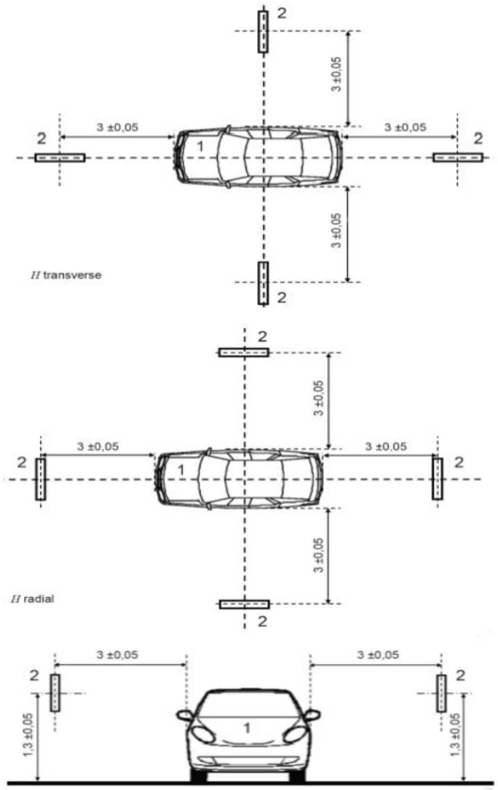

Fig. 1. CISPR 36 [14]. Measurement positions around a car.

Furthermore, the measurement time is for carrying out only one working mode of EUT. Antennas which can measure several orientations at the same time can immediately reduce the measurement time. Since in [3] a high EM field in two polarizations (*X* and *Y* axis) around an EUT was shown, the possibility to have high EM field in third polarization (*Z* axis) is present. Therefore, in order to evaluate emissions from the EUT, all three polarizations should be measured.

With increasing the number of antennas, even to two, the influence on the measurement results could be visible [2]. Evaluation of the two-antenna construction was done by measurements and simulations. Deviations can occur due to the influence of the nearby distance to the additional antenna which has an impact on the measurement results [16]. Orthogonal placed antennas was discussed in [2] provides a possibility to decrease the influence on the measurement results by an additional antenna itself. However, this is only possible if the radiated EM field is co-polarized with one antenna and un-polarized with another. This is typical for antenna factor measurements using another antenna as a reference source [11],[7]. In this case, the antenna which is measuring a lower value of the EM field will have a less influence on the other one. It is due to the fact that the difference of the measured values between *X* and *Y* antenna positions to the transmitting antenna is around 20 – 30 dB [2]. However, based on the research performed in [12], the mutual coupling between antennas will be higher when the measured values in both antennas would be nearly the same. Therefore, the evaluation procedure of the three-antenna construction should take in to account different combinations of EM field propagation in *X, Y*, and *Z* axes.

The mutual coupling between antennas will be due to several reasons. One of them is the close proximity of the antennas in the three-axis antenna setup [16], which will cause an error which could be easily included in the antenna correction factor. Another reason that will have an influence on the mutual coupling between antennas is the value of the EM field which measures each antenna. As described in [12], the mutual coupling between antennas will be stronger if each antennas will measure nearly the same value of the EM field. If the EM field would be strong only on the *X*-axis, antennas that are oriented in *Y*, and *Z* axes will have a minimal influence on the measurement data by the antenna which is oriented on *X*-axis. However, if the EM field propagates with the same level in all three axes, the coupling between antennas will be stronger and the influence of each antenna would be higher. With the known relationship between the EM field value measured by each antenna and the error which can cause each antenna on others, the correction factor can be applied to illuminate the mutual-coupling effect.

Three antennas with different diameters 60 cm, 57 cm, 63 cm, were placed inside each other as shown in Fig. 2. A better version with three loops of 60 cm has been built, but in this paper the older version with three different diameters have been used. Since loop antennas are linearly polarized, a 90-degree rotation between antennas generally would be sufficient to decease the receiving orthogonal polarized field by other antennas. In order to eliminate the influence of the cables of the two antennas which are not used during evaluation procedure, they were terminated by 50-Ohm loads to mimic the termination by a measuring receiver.

A spectrum analyser (SA) was connected to one of the receiving antennas (RX) and a tracking generator (TG) was connected to the transmitting antenna (TX) antenna, allowing to measure the magnitude of the transmission coefficient $|S_{21}|$, as shown in Fig. 3. All data were collected via a laptop and further post-processed in MATLAB.

An anechoic chamber of 4.5 m x 3.5 m x 3 m was used to reduce the influence of the ambient noise by acting as a Faraday cage only, since the absorbers are not effective in this frequency range.

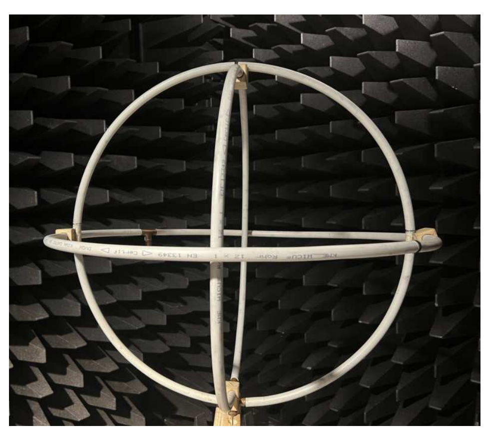

Fig. 2. Three-antenna construction.

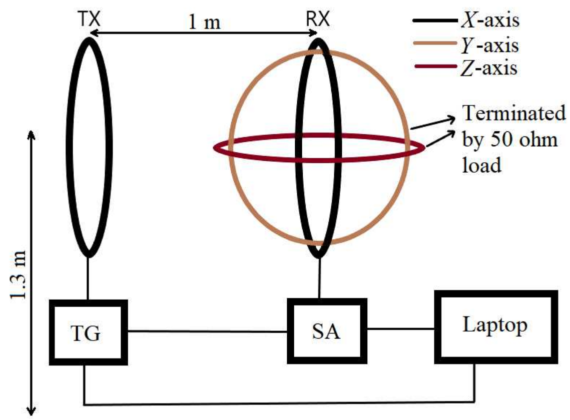

Fig. 3. Three-antenna measurement setup.

According to [9], such a chamber could be successfully used with a minimal influence on the measurement results in the low-frequency range. To minimize the measurement error, the distance from the nearest reflecting object should be from two till three times the antennas separation distance. Due to [9] antenna separation distance of 1 meter was used. A 1.3-meter distance from antennas centre to the ground was used [11]. Because the TX antenna position to the RX during one-, two- and three-antenna construction evaluation procedure is never changed, only the presence of an additional RX antennas is relevant for the measurement results. For one-antenna setup, only a black RX antenna was used, as in Fig. 3. A two-antenna setup – black and orange RX, three-antenna setup – all three antennas were used. X, Y, and Z axes will be used as markers to designate the position of the RX antenna to the TX antenna.

III. Measurement method

Since standard radiated EMI measurement uses one antenna during the evaluation procedure, as a starting point one-antenna construction measurement data is compared to two- and three-antenna construction. In Fig. 4 the antenna positions in the anechoic chamber (AC) during the measurements are shown. Several antenna positions in the AC were measured to verify the difference in the influence of the conducted walls. Antennas were placed in the middle of the AC parallel to the walls, after that RX and TX antenna were shifted on 25 centimetres in one and another direction Fig. 4(*a*). The influence which is caused by changing antenna's positions in the AC will be shown in section IV. Fig. 4(*b*) shows the antennas positions in the AC which will be used for the measurement results analysis in section IV.

After one-antenna measurements in *X* and *Y* antenna positions, the second antenna and the third antenna were added in a row. The same measurements as for one-antenna construction were applied for two- and three-antenna construction. In Section IV only measurement results from *X* and *Y* RX antenna positions for one-, two-, and three-antenna construction will be compared.

In order to evaluate the measurement error which could be caused by nearly the same value of EM field in all three polarizations, the TX antenna was then tilted by 45 degrees in all three *X, Y* and *Z* axes. Fig. 5 shows the position of TX antenna during other one-, two- and three-antenna construction measurements.

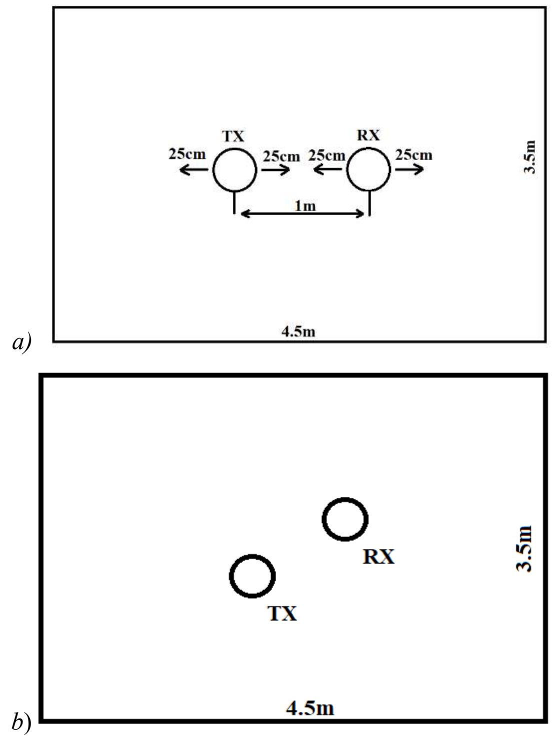

Fig. 4. a) Antenna positions in the anechoic chamber parallel to the walls. b) Antenna positions in the AC for final measurement results top view.

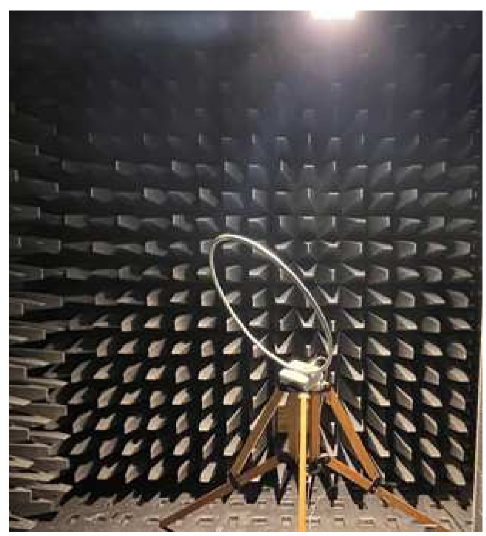

Fig. 5. Transmitting antenna position tilted to 45 degrees in *X, Y,* and *Z* axis.

IV. Measurement Results and Analysis

A. Non-tilted TX antenna position, one antenna construction

The one-antenna construction measurements with non-tilted TX were performed. Fig. 6 presents measurement results from *X* and *Y* RX antenna positions with respect to the TX antenna. Upper part of the graph represents the difference in the measurement results due to the antenna positions in the anechoic chamber. From 500 kHz, the difference between *X* and *Y* antenna positions vary from 15 to 25 dB. *X* antenna results are higher than *Y* antenna results due to the crossisolation factor. *Y* measurement data from one-antenna construction shows the results of the measured $|S_{21}|$ value for orthogonally oriented antenna. Since the standard measurements [14], [15] are focused only on the highest values of the measured radiated EMI only *X* RX antenna positions is evaluated for normal TX antenna position.

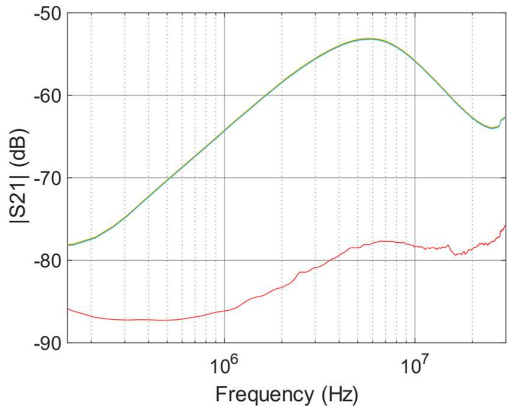

Fig. 6. $|S_{21}|$ results for the *X* RX positions to TX - top curves on the graph with respect to the antenna positions in the AC to show the influence of the conducted walls on the difference in the results. *Y* RX positions to TX – bottom curve.

B. *Not-tilted TX antenna position, two- and three antenna constructions*

After *one-antenna* construction measurements, *two*- and *three-antenna* construction measurements were performed. Fig. 7 shows the measurement results of *X* antenna in one-, two-, and three-antenna construction. Fig. 8 shows the difference in $|S_{21}|$ values between all constructions. The difference in the measurements results after adding the second antenna vary between 0 and 0.2 dB for the whole frequency range. For three-antenna construction, the difference in the measurement results increases in the frequency range above 20 MHz from 0.2 to 0.6 dB. It shows the influence on the measurement data by an additional antenna presence itself. Further this data will be compared to the measurements with tilted TX position. The receiving signal of the orthogonal antennas could be negligible since $|S_{21}|$ from *X* antenna position higher than *Y* antenna position on 15 to 25 dB for the frequency range above 500 kHz (Fig. 8).

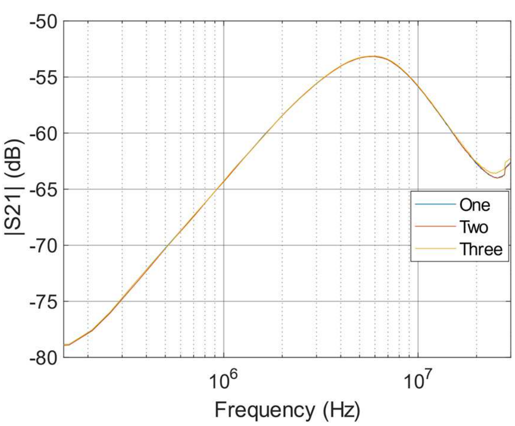

Fig. 7. $|S_{21}|$ results between the 60 cm RX antenna *X* to the TX antenna, in one-, two-, and three- antenna construction.

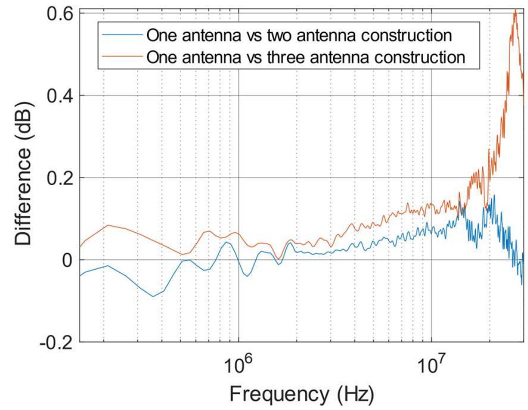

Fig. 8. Difference in the measurement results between one- vs two- and one- *vs* three-antenna construction.

C. *Measurements of one-, two-, and three-antenna construction with tilted TX*

The same measurements which were performed for *one-antenna* construction previously were repeated with tilted TX. From Fig. 9 it is clearly visible that the difference in *X, Y, and Z* RX positions is around 3-4 dB for the whole frequency range, which is pretty close compared to Fig. 6. With more precise TX antenna angle calibration the difference between all of three axis could be eliminated, but it was not the main goal in this paper. It is due to non-directional EM field propagation from TX. This data will be used to calculate the difference in the measurement results for two- and three-antenna constructions with tilted TX. Fig. 10 shows the *Y* measurement results for one-, two-, and three-antenna construction. It is possible to notice that for the frequencies below 20 MHz the difference in the measurement results around 0.1 – 0.2 dB. For frequencies above 20 MHz the difference in the measurement results for two- and three-antenna construction rises to between 1 and 1.8 dB respectively. Fig. 11 shows the difference between one- and two-, and one- and three-antenna constructions. With tilted TX it is clearly visible that for two-antenna construction the difference in the measurement results for the frequencies above 10 MHz increases to 1 dB. The difference for non-tilted TX for two-antenna construction was nearly 0.2 dB (Fig.8). Same increases in the difference can be traced and for three-antenna constructions. The maximal difference in the measurement results caused by a three-antenna construction increase from 0.6 dB with non-tilted TX to 1.8 dB with tilted TX.

Since measured EM field for *X* and *Y* antenna positions for tilted TX is nearly the same, *X* antenna position was also compared. Fig. 12 presents the difference for *X* antenna position for one-, two-, and three-antenna constructions. The difference in the measurements is stable during the whole frequency range and not only for high frequency which was shown before in Fig. 10. Fig. 13 represents the difference in the measurement results between one- vs two-, one- vs three-antenna construction. From Fig. 13 could be concluded that due to the nearly same level of the measured EM field by each antenna the mutual coupling between antennas which create the difference in the measurement results became stronger. The impact which produce an antenna with higher measured value will be dominant above other antennas. The difference between one- and three-antenna construction was around

3 dB, but only at the very end of the frequency range. The difference below 20 MHz was shown to be consistently around 0 dB for all analysed cases showing that only a negligible difference is to be expected from a three-axis antenna setup. Such a very small difference is supposed to be caused by the imperfect antenna's orientation with respect to each other, and is expected to be minimized if care is taken to manufacture such an antenna more carefully.

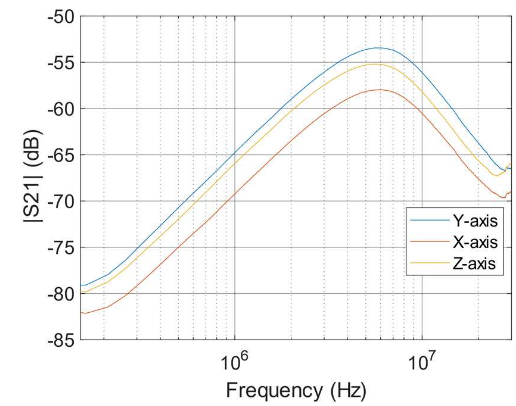

Fig. 9. $|S_{21}|$ results between one-antenna construction with tilted TX antenna for *X*, *Y*, and *Z* axes.

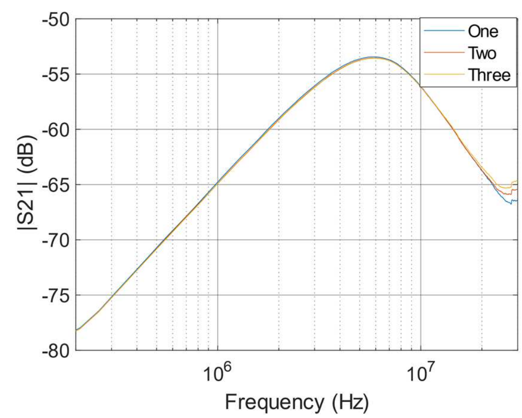

Fig. 10. $|S_{21}|$ results between the RX antenna for *Y*-axis to the tilted TX antenna, for one-, two-, and three-antenna construction.

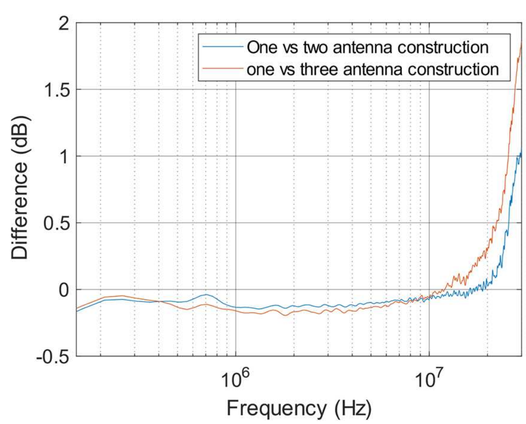

Fig. 11. Difference for *Y* measurements between one, two, and three-antennas construction with tilted TX.

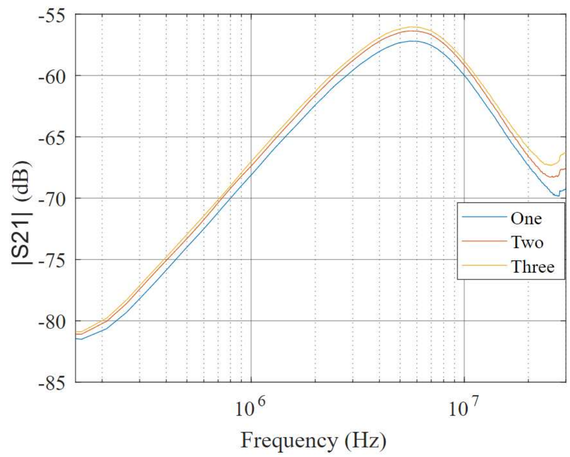

Fig. 12. $|S_{21}|$ for one-, two-, and three-antenna construction with tilted TX for *X*-axis antenna measurements.

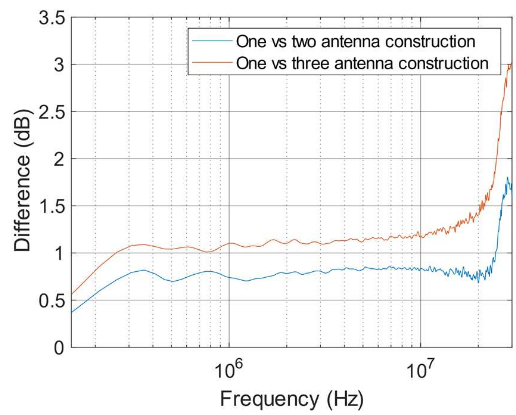

Fig. 13. Difference in the measurement results between one vs two and one vs three-antenna construction for *X*-axis.

V. Conclusion

In order to utilize the decreased measurement time for standard radiated EMI measurements below 30 MHz the mutual coupling between three orthogonal antennas was investigated. A polarized EM field, as normally used during antenna correction factor measurements, and an EM field with has nearly the same value in all of three polarizations were used during this research. The one-antenna construction, which is used for standard measurements, was taken as a reference and was compared to two- and three-antenna construction. The measurement results with the polarized field in one polarization for two- and three-antenna construction shows that the influence of the presence of an additional antenna could be nearly 0 dB for the frequency range below 20 MHz, compared to the one-antenna. For the upper frequencies, above 20 MHz, the difference increased to 0.6 dB for the three-antenna construction. To achieve nearly the same value of EM field in all of three polarizations, the transmitting antenna was tilted in *X*, *Y* and *Z* direction. Comparing the results show that the mutual coupling between antennas could be stronger depending on the measured value of each antenna. With nearly the same measured results for all three antennas, the difference between one and three antenna construction increased by 1 dB for the frequency range below 20 MHz. For the frequency range above 30 MHz, the difference was around 2-3 dB.

The mutual coupling between antennas which is represented by close proximity could be even smaller with a more carefully antenna manufacture.

For future research, the dependence between frequency and measured value by each antenna and the mutual-coupling which is based on it will be investigated. It will create the possibility to provide accurate measurements with three-antenna constructions using a variable correction factor.

REFERENCES

[1] K. Pliakostathis, M. Zanni, G. Trentadue, H. Scholz, “Vehicle electromagnetic emissions: challenges and considerations,” 2019 International Symposium on Electromagnetic Compatibility – EMC EUROPE, 2-6 Sept. 2019, DOI: 10.1109/EMCEurope.2019.8871957.

[2] D. Pokotilov, R. Vogt-Ardatjew, F. Leferink, “Efficient multichannel time-domain multiaxis loop antenna measurement for frequencies below 30 MHz,” 2021 IEEE International Joint EMC/SI/PI and EMC Europe Symposium, 26 July – 13 Aug. 2021, DOI: 10.1109/EMC/SI/PI/EMCEurope52599.2021.9559156.

[3] F. Silva, M. Aragon, “Electromagnetic interferences from electric/hybrid vehicles”, 2011 XXXth URSI General Assembly and Scientific Symposium, 13-20 Aug. 2011, DOI: 10.1109/URSIGASS.2011.6050737

[4] M.S. Alamsyah, F.L. Vieira, H. Garbe, S. Koj, “The effect of stray capacitance to the common mode current on three-phase system,” 2021 IEEE International Joint EMC/SI/PI and EMC Europe Symposium, 26 July – 13 Aug. 2021, DOI: 10.1109/EMC/SI/PI/EMCEurope52599.2021.9559135

[5] S. Koj, S. Fisahn, H.Garbe, “Determination of radiated emissions from wind energy conversion systems,” 2016 International Symposium on Electromagnetic Compatibility - EMC EUROPE, 5-9 Sept. 2016, DOI: 10.1109/EMCEurope.2016.7739262

[6] M. Pous, M. Azpúrua and F. Silva, "Benefits of full time-domain EMI measurements for large fixed installation", 2016 International Symposium on Electromagnetic Compatibility - EMC EUROPE, pp. 514-519, 2016.

[7] D. Pokotilov, R. Vogt-Ardatjew, F. Leferink, “Efficient time-domain multi-channel measurements using a multi-axis antenna for frequency range below 30 MHz,” 2021 Asia-Pacific International Symposium on Electromagnetic Compatibility (APEMC), 27-30 Sept. 2021, DOI: 10.1109/APEMC49932.2021.9597154

[8] J.R. Bergervoet, H.V.Veen. “A large-loop antenna for magnetic field measurements,” Proc. Zurich Int. Symp. EMC. 1989, Zurich, Switzerland, Jan. 1989, pp. 29-34

[9] M. Savi, T.Z. Gireli, F.A. Tirich, C.A.F. Sartoni, “Developing a Van-Veen and Bergervoet antenna,” 2004 International Symposium on Electromagnetic Compatibility, 9-13 Aug. 2004, DOI:10.1109/ISEMC.2004.1349889

[10] R. IJzereef, "Design construction and evaluation of a 3D loop antenna", final M.Sc. assighnment, University of Twente, Enschede, The Netherlands, 2019.

[11] M.J. Alexander, M.J. Salter, D.G. Gentle, D.A. Knight, B.G. Loader, K.P. Holland, “Measurement good practice guide №73. Calibration and use of antennas, focusing on EMC applications,” National physical laboratory, Teddington, UK, Dec. 2004, p.p. 70, available online: https://www.npl.co.uk/special-ages/guides/gpg73_antennas.pdf

[12] A.G. Fotev, B.D. Popovic, “Mutual influence of two close perpendicular wires with pulse excitations,” 1991 Seventh International Conference on Antennas and Propagation, ICAP 91 (IEE), 15-18 April 1991, available online: https://ieeexplore.ieee.org/document/98309

[13] K. Pliakostathis, M. Zanni, G. Trentadue, H. Scholz, “Assessment of a Vehicle’s electromagnetic emissions under dynamic drive conditions,” IEEE Transactions on Electromagnetic Compatibility col. 62, issue: 6, Dec. 2020, pp. 2411-2422, 2020, DOI: 10.1109/TEMC.2020.2968140

[14] "CISPR 36:2020 Electric and hybrid electric road vehicles – Radio disturbance characteristics – Limits and methods of measurement for the protection of off-board receivers below 30 MHz", *IEC*, 07 2020.

[15] CISPR 12, Vehicles', motorboats' and spark-ignited engine-driven devices' radio disturbance characteristics - Limits and methods of measurement, 5th edition 2001 and Amd1: 2005, International Standard.

[16] P.A. Beeckman, "The influence of positioning tables on the results of radiated EMC measurements", 2001 IEEE EMC International Symposium, pp. 280-285, 13 – 17 Aug. 2001.

[17] A. Sen, S. Cakir, T. Pavlíček, “Traceable loop antenna calibration methods using a VNA,” Activity report, 2020, available online: http://www.rfmw.cmi.cz/documents/deliverables/Traceable_loop_antenna_calibration_VNA.pdf